

# The Role of Spatial Potential Fluctuations in the Shape of the PL Bands of Multinary Semiconductor Compounds

J. Krustok,<sup>1</sup> H. Collan,<sup>2</sup> M. Yakushev<sup>3</sup> and K. Hjelt<sup>2,4</sup>

<sup>1</sup> Tallinn Technical University, Ehitajate tee 5, Tallinn 0026, Estonia\*

<sup>2</sup> Optoelectronics Laboratory, Helsinki University of Technology, P.O. Box 3000, FIN-02015, Espoo, Finland

<sup>3</sup> Department of Physics, University of Salford, Salford, M5 4WT, U.K.

<sup>4</sup> Present address: Electronic Instrumentation Lab., DIMES, Delft University of Technology, Makelweg 4, 2628 CD Delft, The Netherlands

Received June 8, 1998; accepted August 6, 1998

PACS Ref: 78.55

## Abstract

Photoluminescence (PL) measurements of  $\text{CuIn}_{1-x}\text{Ga}_x\text{Se}_2$  ( $x = 0.5$ ) single crystals grown by the vertical Bridgmann technique were made at temperatures ranging from 11 K to 200 K and with various excitation powers. At low temperatures only one asymmetric PL band (BT-band) is present at 1.23 eV. It has a steeper decline on the high-energy side and nearly temperature independent low-energy side. At higher temperatures ( $T > 140$  K) the BB-band becomes visible at 1.31 eV. We used an asymmetric double sigmoidal function to fit the experimental PL spectra. The results of this fitting can be interpreted to show the presence of spatial potential fluctuations in our samples. Observed dependencies would seem to reveal that the BT band is indeed connected with the recombination of a free electron with a localized hole. It is shown that these relatively deep localized states are probably formed due to potential fluctuations in highly compensated material and are not connected with any particular acceptor defect. We show that this model conforms to most of the discovered dependencies.

## 1. Introduction

For the solution of environmental and resources problems, a solar cell technology using multinary chalcopyrite semiconductors, especially  $\text{CuIn}_x\text{Ga}_{1-x}\text{Se}_2$  (CIGS), has made rapid progress. Understanding the behavior of intrinsic defects in CIGS is significant to further improve of CIGS-based solar cells. The photoluminescence (PL) has proved to be the most powerful technique in defect studies. The general characteristics, such as the shape, of the PL emission bands of these compounds are highly sensitive to the composition of the samples. This makes an unambiguous interpretation of experimental PL information extremely difficult and, in fact, seems to have resulted in the publication of misleading findings. The most efficient solar cells are obtained using In-rich CIGS absorber layers, but In-rich CIGS, in particular, usually shows broad and asymmetric PL band without any clear phonon structure [1, 2]. Due to its visible blue shift with excitation intensity ( $j$ -shift) this band is often thought to be a donor-acceptor pair (DAP) band. But the magnitude of the observed  $j$ -shift usually exceeds the typical energy shift for DAP band. Therefore, there is a clear need to investigate, in detail, the shape of the PL bands in In-rich CIGS and to find some reasonable theoretical background for the processes affecting the shape of the bands.

## 2. Theoretical background

The bandgap energy of ternary compounds is highly sensitive to the stoichiometry and, thus, spatial fluctuations in composition also cause fluctuations of the bandgap energy [3]. This is one possible reason for the widening of the PL bands. The second reason may be connected with the high concentration of defects in highly compensated CIGS samples. The fluctuations of defect potentials cause widening of the defect levels within the forbidden gap of CIGS and so-called band tails are formed. Spatial potential fluctuations are quite common in highly doped and compensated semiconductors [4, 5], for which the theory describing the electrical and optical properties was developed by Shklovskii and Efros [6], and by Levanyuk and Osipov [7]. It was shown that the edge emission in highly compensated semiconductors essentially includes two typical emission bands: the band to tail (BT) and the band to band (BB) bands, shown schematically in Fig. 1. The BT-band usually dominates at low temperatures while the BB-band becomes visible at high temperature and at high excitation intensities [7]. Due to the potential fluctuations at low temperatures the holes are mostly captured by deep band states within the fundamental energy gap. These deep band states form localized states for holes which look more like acceptor

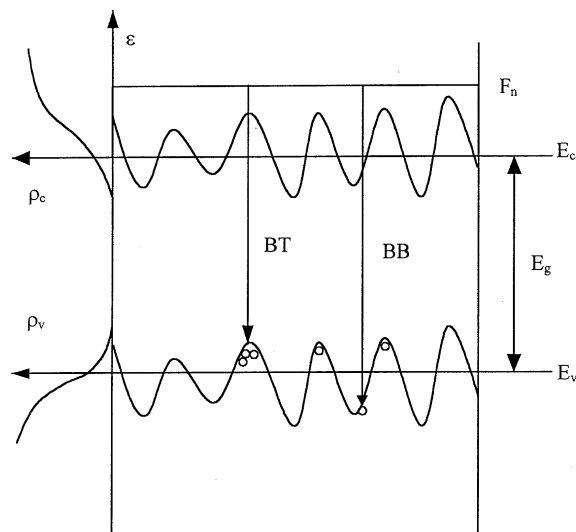


Fig. 1. Schematic representation of the PL transitions in  $\text{CuIn}_x\text{Ga}_{1-x}\text{Se}_2$ . The BT and the BB bands typically overlap each other, the former being dominant at low temperature and the latter dominant at high temperature.

\* E-mail: krustok@cc.ttu.ee

states rather than valence band states. In order to find the shape of the corresponding BT-band it is necessary to use a density of states function and a distribution function for both electrons in the conduction band and localized holes [7]:

$$I_{\text{BT}}(h\nu) \propto \int \int W_{\text{BT}}(E_e, E_h) \rho_c(E_e) f_e(E_e) \rho_v(E_h) q_h(E_h) \times \delta(E_e - E_h - h\nu) dE_e dE_h, \quad (1)$$

where  $W_{\text{BT}}$  is a radiative recombination probability,  $E_e$ ,  $E_h$ -energy of electrons and holes, respectively,  $\rho_c$ ,  $\rho_v$ -density of states function for the electrons in the conduction band and for the localized holes, respectively,  $f_e$ -distribution function for the electrons,  $q_h$ -distribution function for the localized holes. The  $q_h$  function must be calculated using kinetic equations rather than assuming that there is a quasi-equilibrium of holes with corresponding quasi Fermi level. The latter assumption is correct, of course, in case of free holes, i.e. for the BB-band. The final shape of the PL band depends crucially on the actual shape of the density of states function for the localized holes and therefore it is difficult to find any analytical function for the BT-band shape. In [8] some predictions were made using different functions for  $\rho_v$  in degenerate semiconductors. This assumption may be correct also for CIGS and related compounds because of the smallness of the effective mass of the electrons (in  $\text{CuInSe}_2$   $m_n = 0.09 m_e$  [9]). The Fermi level for electrons  $F_n$  lies then in the conduction band and the electron part of the integral (1) is the same for all types of  $\rho_v$ . According to [8] the resulting BT-band at low temperatures has an asymmetrical shape with an abrupt decrease on the high-energy side. The low-energy side of this band is determined by the  $\rho_v$  function while the high-energy side has much more complex nature. It is obvious that the shape of the low-energy side of the BT-band should not depend on temperature and excitation intensity. In most cases  $\rho_v$  and the emission intensity on the low-energy side  $I_{\text{LE}}$  at low temperatures have the following shapes:

$$\rho_v(\varepsilon) = \rho_0 \exp\left(-\frac{\varepsilon}{\gamma_0}\right), \quad (2)$$

$$I_{\text{LE}}(h\nu) \propto \exp\left[-\frac{E_g - h\nu}{\gamma_0}\right]. \quad (3)$$

If the radiative recombination probability  $W_{\text{BT}}$  has a steeper dependence on electron and hole energy, a small temperature dependence of  $I_{\text{LE}}$  may be expected [7]. At the same time the intensity on the high-energy side  $I_{\text{HE}}$  of the BT-band has several common properties for all types of the density of states function for localized holes. At low temperatures ( $kT < \gamma_0$ ) the curvature of  $I_{\text{HE}}(h\nu)$  does not depend on temperature but at higher temperatures ( $kT > \gamma_0$ ) its slope decreases linearly with temperature and the BT-band becomes more symmetrical. The slope of  $I_{\text{HE}}(h\nu)$  decreases with excitation power at the low-temperature region.

The easiest way to track the properties of the BT-band is to find its maximum energy  $h\nu_{\text{max}}$  and study its temperature and excitation intensity dependencies. According to [7, 8] the  $h\nu_{\text{max}}$  for BT-band at low temperatures may be expressed as:

$$h\nu_{\text{max}} = h\nu_{\text{max}}^0 - \varepsilon_1, \quad (4)$$

where

$$\varepsilon_1 = kT \ln \frac{N_V}{p + n\Theta}, \quad (5)$$

$N_V$ -effective density of states in the valence band,  $n$ ,  $p$ -concentration of free electrons and holes, respectively,  $\Theta$ -ratio of electron and hole capture probabilities by localized state. Thus, the BT-band may be treated as a recombination of a free electron from Fermi level  $F_n$  with a hole, captured by the localized state with depth  $\varepsilon_1$ . According to eqs (4) and (5) at low temperatures  $h\nu_{\text{max}}$  decreases linearly with temperature and more rapidly than the energy gap. As it can be seen from eqs (4) and (5) and  $h\nu_{\text{max}}$  also shifts toward higher energies with increasing  $n$  and  $p$ , i.e. with excitation intensity. At higher temperatures, when

$$kT > kT_1 = \gamma_0 \left[ \ln \frac{N_V}{p + n\Theta} \right]^{-1/2} \quad (6)$$

$h\nu_{\text{max}}$  shifts toward higher energies until above some characteristic temperature  $T_2$  it will follow the temperature dependence of the energy gap. At temperatures where all localized holes are thermally released the BB-recombination dominates.

### 3. Experimental

The  $\text{CuIn}_x\text{Ga}_{1-x}\text{Se}_2$  ( $x = 0.5$ ) single crystals were grown by the vertical Bridgmann technique. For the PL measurements, a 5 mW He-Ne laser beam with a wavelength of 632.8 nm was used for excitation. The excitation spot size was about 1 mm. The CIGS sample with freshly cleaved surface was mounted in a closed-cycle He cryostat capable of cooling down to 11 K. A computer-controlled SPEX 1870 grating monochromator (0.5 m) with a spectral resolution of 0.5 nm was used in PL measurements. The chopped signal was detected with a liquid-nitrogen cooled Ge detector using a conventional lock-in technique. For the purpose of analysis, the emission spectra were corrected for grating efficiency variations and for the spectral response of the detector, which were calibrated separately. The PL measurements were made at temperatures ranging from 11 K to 200 K and with various excitation powers.

### 4. Results and discussion

At low temperatures only one asymmetric PL band (BT-band) is present with  $h\nu_{\text{max}} = 1.23$  eV. Just as predicted by theory [6–8], it has a steeper decline at high-energy side and a nearly temperature independent shape at the low-energy side, see Fig. 2. At higher temperatures ( $T > 130$  K) a new PL band (BB-band) appears, centered at  $h\nu = 1.31$  eV. In order to simplify the following of the changes in the PL-bands shape all the experimental spectra were fitted with an empirical asymmetric double sigmoid function:

$$I(h\nu) = A \left( 1 / \left( 1 + \exp \left[ -\frac{h\nu - E_1}{W_1} \right] \right) \right) \times \left( 1 - 1 / \left( 1 + \exp \left[ -\frac{h\nu - E_2}{W_2} \right] \right) \right). \quad (7)$$

Here  $A$ ,  $E_1$ ,  $E_2$ ,  $W_1$  and  $W_2$  are the experimental parameters. Parameters  $E_1$  and  $W_1$  represent the shape of the low-energy side of the PL bands while  $E_2$  and  $W_2$  belong to the

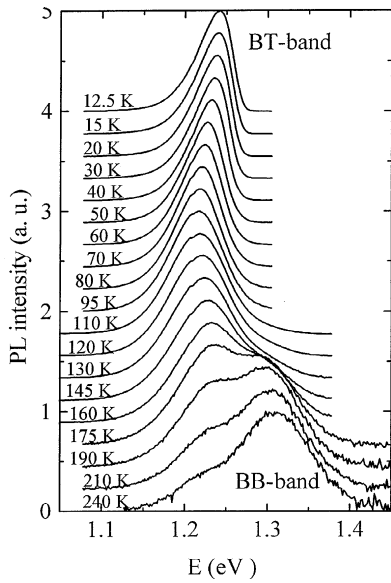


Fig. 2. Normalized PL spectra of  $\text{CuIn}_x\text{Ga}_{1-x}\text{Se}_2$  measured at different temperatures.

high-energy side. This fitting function is purely empirical and was chosen from among several candidates because it always seemed to give the best result. According to the theory, eqs (2) and (3), the nearly exponential low-energy side of the BT band indicates that the hole distribution function in the forbidden gap  $\rho_v(E_h)$  has also an exponential shape.

Temperature dependence of the peak position for both bands is depicted in Fig. 3. It is clearly visible that at low temperatures the peak position of the BT-band shifts towards low energies linearly with temperature according to eq. (4). This is a temperature region where the energy gap  $E_g$

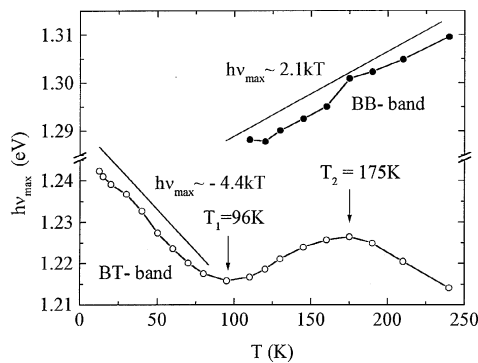


Fig. 3. Temperature dependence of the BT- and BB-bands peak positions. Solid lines represent linear sections with the corresponding slopes given.

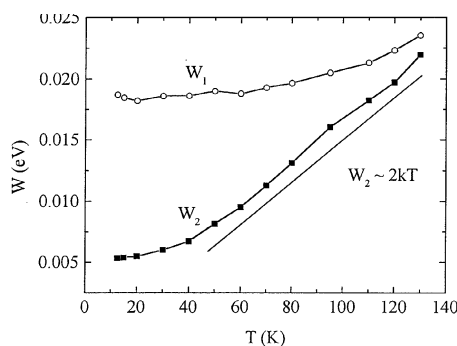


Fig. 4. Temperature dependence of fitting parameters  $W_1$  and  $W_2$  obtained from the fitting of the BT-band with eq. (7).

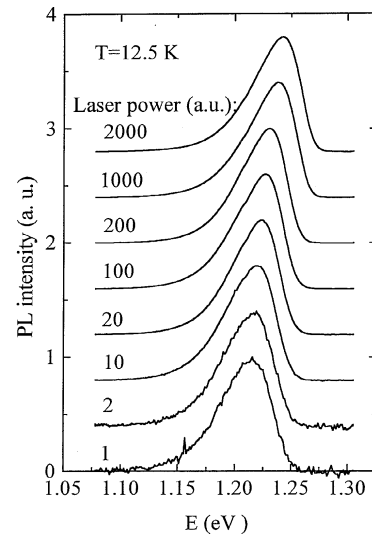


Fig. 5. Normalized PL spectra of the  $\text{CuIn}_x\text{Ga}_{1-x}\text{Se}_2$  BT-band with different excitation power.

has usually very slow temperature dependence and therefore it is appropriate to write according to eq. (5):

$$\ln \frac{N_v}{p + n\Theta} = 4.4. \quad (8)$$

In accordance with the theory, there is a minimum at  $T_1 = 96 \text{ K}$ , see Fig. 3. From eqs (6) and (8) we get  $\gamma_0 = 17 \text{ meV}$ . The last value is verified in Fig. 4, where the fitting results for the BT-band are presented. We can see, that at low temperatures the  $W_1$  parameter has a value very close to the  $\gamma_0$  value of 17 meV and, as predicted by the theory,  $W_1$  does not change much with temperature. At the same time the  $W_2$  value increases with temperature as  $W_2 \sim 2kT$  and finally at high temperatures ( $T \approx 140 \text{ K}$ ) both parameters become nearly equal. This means that BT-band will have a symmetrical shape. All these features were predicted by the theory [7, 8].

At still high temperatures the BB-band emerges and its peak position shifts towards higher energy. As it was found in [7], this kind of shift is possible in degenerate semiconductors, where

$$h\nu_{\text{max}}^{\text{BB}}(T) \sim E_g^*(T) - kT \ln \left( \frac{2(F_n - E_c)}{kT} \right). \quad (9)$$

To satisfy the experimentally found dependence  $h\nu_{\text{max}}(T) \sim 2.1kT$  (see Fig. 3) it is obvious, that the value of  $F_n - E_c$  in

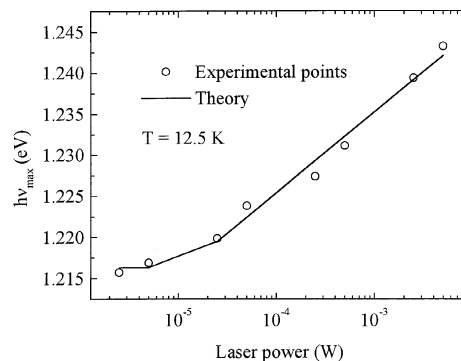


Fig. 6. The dependence of the peak position of the BT-band on excitation power and the theoretical fit using eq. (11).

eq. (9) must be quite small and, in fact, not exceed 2–3 meV. Therefore we may assume, that for the present sample the Fermi level  $F_n$  lies very close to the conduction band edge. The temperature dependence of  $E_g$  for  $\text{CuIn}_x\text{Ga}_{1-x}\text{Se}_2$  ( $x = 0.5$ ) is not known, but we may use data obtained for  $\text{CuInSe}_2$  and  $\text{CuGaSe}_2$  in [10]. In this paper it was shown that  $dE_g/dT$  values are  $-0.9 \times 10^{-4}$  and  $-1.1 \times 10^{-4}$  eV/K for  $\text{CuInSe}_2$  and  $\text{CuGaSe}_2$ , respectively. For  $\text{CuIn}_x\text{Ga}_{1-x}\text{Se}_2$  ( $x = 0.5$ ) obviously this value must be between these two values, i.e.  $1.0 \text{ k} < |dE_g^*/dT| < 1.28 \text{ k}$ . According to [8]

$$T_2 = \frac{\gamma_0}{k\sqrt{\beta}}, \quad (10)$$

where  $\beta = |dE_g^*/dT|/k$ . Using experimentally obtained values  $T_2 = 175 \text{ K}$  and  $\gamma_0 = 17 \text{ meV}$  we get from eq. (10)  $\beta \approx 1.27$ . Although this value is quite rough it lies within the expected region.

Figure 5 shows the BT-band shape with increasing excitation laser power at 12.5 K. The BT-band shifts towards higher photon energies with increasing excitation intensity ( $j$ -shift), see also Fig. 6. At the same time the shape of the BT-band does not change remarkably. The  $j$ -shift of the BT-band, according to eqs (4) and (5), is determined by increasing of the denominator in eq. (5),  $\eta = (p + n\ominus)$ , with excitation intensity  $J$ . The dependence of  $\eta$  upon  $J$  is not straightforward, but in many cases it can be presented as a power function:  $\eta = \eta_0 + \sigma J^\alpha$ . Then we get from eq. (4):

$$h\nu_{\max}^{\text{BT}}(J) = h\nu_{\max}^0 - kT \ln \frac{N_V}{\eta_0 + \sigma J^\alpha}. \quad (11)$$

The fitting with eq. (11) is also shown in Fig. 6 as a continuous line. The best fit was found with  $h\nu_{\max}^0 = 1.268 \text{ eV}$ ,  $N_V = 4.53 \times 10^{18} \text{ cm}^{-3}$ ,  $\eta_0 = 8.5 \times 10^{-3} \text{ cm}^{-3}$ ,  $\sigma = 2.9 \times 10^{17} \text{ cm}^{-3}$  and  $\alpha = 4$ .

## 5. Conclusions

We have studied experimentally the photoluminescence of  $\text{CuIn}_x\text{Ga}_{1-x}\text{Se}_2$  ( $x = 0.5$ ) as a function of temperature and of excitation intensity and done a detailed analysis of the band shape for the BT (1.23 eV) and BB (1.31 eV) PL bands. Observed dependencies reveal that the BT band is indeed connected with the recombination of a free electron with a localized hole. It is shown that these relatively deep localized states are probably formed due to potential fluctuations in highly compensated material and are not connected with any particular acceptor defect. The genuine BB-band becomes visible only at higher temperatures,  $T > 140 \text{ K}$ , and is probably related to the free electron–free hole recombination.

## Acknowledgements

This work was supported by the Estonian Scientific Foundation grant No. 3417.

## References

1. Masse, G., Djessas, K. and Guastavino, F., *J. Phys. Chem. Solids* **52**, 999 (1991).
2. Dirnstorfer, I. *et al.*, *Inst. Phys. Conf. Ser.* No 152, 233 (1998).
3. Schlicht, F. *et al.*, *Cryst. Res. Technol.* **31S**, 745 (1996).
4. Krustok, J. and Kukk, P. E., *Mat. Sci.* **15**, 43 (1989).
5. Shen, W. Z. *et al.* *Infrared Phys. Technol.* **37**, 509 (1996).
6. Shklovskii, B. I. and Efros, A. L., "Electronic Properties of Doped Semiconductors" (Springer, Berlin, 1984).
7. Levanyuk, A. P. and Osipov, V. V., *Sov. Phys. Usp.* **24**, 187 (1981).
8. Levanyuk, A. P. and Osipov, V. V., *Sov. Phys. Semicond.* **7**, 721 (1973).
9. Rincon, C. and Sanchez Perez, G., *Progr. Cryst. Growth Charact.* **10**, 307 (1984).
10. Mudryi, A. V. *et al.*, *Solar Energy Mater. Solar Cells.* **53**, 247 (1998).